ANOMALOUS DIFFUSION AND HEAT TRANSFER ON COMB STRUCTURE WITH ANISOTROPIC RELAXATION IN FRACTAL POROUS MEDIA

by

Zhaoyang WANG[a], Liancun ZHENG[a,*], Lianxi MA[b], and Goong CHEN[c]

[a] School of Mathematics and Physics, University of Science and Technology Beijing, Beijing, China
[b] Department of Physics, Blinn College, Bryan, Tex., USA
[c] Department of Mathematics and Institute for Quantum Science and Engineering, Texas A&M University, College Station, Tex., USA

Original scientific paper
https://doi.org/10.2298/TSCI200113153W

A kind of anomalous diffusion and heat transfer on a comb structure with anisotropic relaxation are studied, which can be used to model many problems in biologic and nature in fractal porous media. The Hausdorff derivative is introduced and new governing equations is formulated in view of fractal dimension. Numerical solutions are obtained and the Fox H-function analytical solutions is given for special cases. The particles spatial-temporal evolution and the mean square displacement vs. time are presented. The effects of backbone and finger relaxation parameters, and the time fractal parameter are discussed. Results show that the mean square displacement decreases with the increase of backbone parameter or the decrease of finger relaxation parameter in a short of time, but they have little effect on mean square displacement in a long period. Particularly, the mean square displacement has time dependence in the form of $t^{\alpha/2}$ $(0 < \alpha \leq 1)$ *when* $t > \tau$*, which indicates that the diffusion is an anomalous sub-diffusion and heat transfer.*

Key words: *Hausdorff derivative, anomalous diffusion and heat transfer, particles transport, mean square displacement, anisotropic relaxation*

Introduction

The classical comb model has been used to describe many abnormal diffusion and heat transfer phenomena in fractal porous media [1, 2]. For example, it has been used to describe the transport of cancer cells [3, 4], the propagation of actin polymerization-reaction [5], the nerve transport along spiny dendrites [6], and quantum non-linear Schrodinger lattices [7]. Iomin [8] and Sandev [9] considered the diffusion and heat transfer of comb structure from a fractal perspective, which can be used to represent more realistic models for describing transport properties, such as infiltration of diffusing and heat transfer of particles from one material to another [10], and diffusion and heat transfer of active species in porous media [11].

Chen and Liang [12] proposed to apply the Hausdorff fractal derivative to describe anomalous diffusion and heat transfer behavior. Cai *et al.* [13] studied the 3-D anomalous diffusion and heat transfer in fractal isotropic/anisotropic porous media by Hausdorff derivative

* Corresponding author, e-mail: liancunzheng@ustb.edu.cn

model and presented a comprehensive physical interpretation. More recent experimental results of solute transport and ultraslow diffusion agree well with the method [14, 15]. Different from most previous studies, in this paper, we introduce the Hausdorff fractal derivative with the time parameter α to study the anomalous diffusion phenomenon on the comb structure, fig. 1

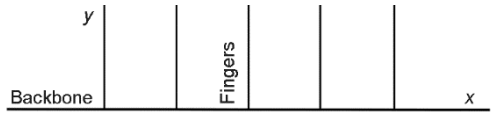

Figure 1. Schematic of the comb structure

The mass conservation equation is written:

$$\frac{\partial P}{\partial t^{\alpha}} = \frac{1}{\alpha t^{\alpha-1}} \frac{\partial P}{\partial t} = -\nabla \vec{\mathrm{J}} \tag{1}$$

where $\vec{\mathrm{J}}$ is the diffusion flux vector, $P = P(t, x, y)$ – the mass distribution function at the time t and the positions (x, y), parameter $\alpha \in (0,1]$ is the time fractal dimension.

It is well known that the classical Fick's model contains paradox with infinite propagation velocity [16, 17]. Cattaneo model [18] overcomes the shortcoming of the Fick's first law of diffusion and heat transfer by introducing the relaxation time term. In many cases, the characteristics of particles diffusion and heat transfer are different due to the different media of the backbone and branches. Fan *et al.* [19] studied anomalous diffusion and heat transfer in circular comb-like structure with anisotropic relaxation in angular as well as in radial direction. Similarly, we need to use different relaxation parameters to describe the diffusion and heat transfer of particles in different directions. The modified constitutive equations are:

$$J_x + \tau_1 \frac{\partial J_x}{\partial t} = -D_1 \frac{\partial P}{\partial x} \delta(y) \tag{2}$$

and

$$J_y + \tau_2 \frac{\partial J_y}{\partial t} = -D_2 \frac{\partial P}{\partial y} \tag{3}$$

where τ_1 is the backbone relaxation parameter and τ_2 is the finger relaxation parameter, respectively.

The initial conditions are:

$$P(0, x, y) = \delta(x)\delta(y) \tag{4}$$

$$J_x(0, x, y) = J_y(0, x, y) = 0 \tag{5}$$

and the boundary conditions are:

$$P(t, \pm\infty, y) = P(t, x, +\infty) = 0 \tag{6}$$

$$\frac{\partial P}{\partial y}(t, x, -\varepsilon) = 0 \tag{7}$$

where $\varepsilon > 0$ is arbitrarily tiny constant, it is used to accommodate the conditions of delta function.

By introducing dimensionless quantities for unification:

$$t \to \frac{D_1^2}{D_2^3} t^*, x \to \frac{D_1}{D_2} x^*, \quad y \to \frac{D_1}{D_2} y^*, \quad \tau_1 \to \frac{D_1^2}{D_2^3} \tau_1^*, \quad \tau_2 \to \frac{D_1^2}{D_2^3} \tau_2^*,$$

$$J_x \to \frac{D_2^4}{D_1^3} J_x^*, \quad J_y \to \frac{D_2^4}{D_1^3} J_y^*, \quad P \to \frac{D_2^2}{D_1^2} P^*$$

We rewrite the governing equations and corresponding initial and boundary conditions in dimensionless forms. For simplicity, the superscript * is omitted:

$$\frac{\partial P}{\partial t} = -\alpha t^{\alpha-1} \nabla \vec{\mathrm{J}} \tag{8}$$

$$J_x + \tau_1 \frac{\partial J_x}{\partial t} = -\frac{\partial P}{\partial x} \delta(y) \tag{9}$$

$$J_y + \tau_2 \frac{\partial J_y}{\partial t} = -\frac{\partial P}{\partial y} \tag{10}$$

$$P(0, x, y) = \delta(x)\delta(y), \quad J_x(0, x, y) = J_y(0, x, y) = 0 \tag{11}$$

$$P(t, \pm\infty, y) = P(t, x, +\infty) = 0, \quad \frac{\partial P}{\partial y}(t, x, -\varepsilon) = 0 \tag{12}$$

Obviously, eqs. (8)-(10) are generalization of the classical diffusion equation, and the solutions become hyperbolic which has a wave-like behavior.

Numerical simulation

In this section, the finite volume method is applied which has conservative characteristic. Due to the symmetry of the region, we consider the diffusion on $(x, y) \in [0,6] \times [0,6]$. This consideration is reflected in the processing of the initial conditions. We set $N_x + 1$ and $N_y + 1$ nodes on the *x*-axis and *y*-axis, respectively, with equal distance. Finally, we let $N_x = N_y = 80$ and $\Delta t = 10^{-5}$.

Discretization scheme of diffusion equation

For the inner nodes, namely $2 \le i \le N_x$ and $2 \le j \le N_y$, the discretization scheme is:

$$P_{i,j}^{k+1} = P_{i,j}^k + \frac{\{(k\Delta t)^\alpha - [(k-1)\Delta t]^\alpha\}}{\Delta x} (Je_{i-1,j}^k - Je_{i,j}^k) + \\ + \frac{\{(k\Delta t)^\alpha - [(k-1)\Delta t]^\alpha\}}{\Delta y} (Jn_{i,j-1}^k - Jn_{i,j}^k) \tag{13}$$

where *Je* is increased flux transport from controlled volume (i, j) to its eastern $(i+1, j)$ and *Jn* is increased flux transport from controlled volume (i, j) to its northern $(i, j+1)$.

For the nodes on boundary $y = 0$, when $2 \le i \le N_x$, we have:

$$P_{i,1}^{k+1} = P_{i,1}^k + \frac{\{(k\Delta t)^\alpha - [(k-1)\Delta t]^\alpha\}}{\Delta x} (Je_{i-1,1}^k - Je_{i,1}^k) - \frac{2\{(k\Delta t)^\alpha - [(k-1)\Delta t]^\alpha\}}{\Delta y} Jn_{i,1}^k \tag{14}$$

Similarly, for the nodes on boundary $x = 0$, when $2 \le j \le N_y$, we have:

$$P_{1,j}^{k+1} = P_{1,j}^{k} - \frac{2\{(k\Delta t)^{\alpha} - [(k-1)\Delta t]^{\alpha}\}}{\Delta x} Je_{1,j}^{k} + \frac{\{(k\Delta t)^{\alpha} - [(k-1)\Delta t]^{\alpha}\}}{\Delta y} (Jn_{1,j-1}^{k} - Jn_{1,j}^{k}) \quad (15)$$

For corner points, we have discretization scheme:

$$P_{1,1}^{k+1} = P_{1,1}^{k} - \frac{2\{(k\Delta t)^{\alpha} - [(k-1)\Delta t]^{\alpha}\}}{\Delta x} Je_{1,1}^{k} - \frac{2\{(k\Delta t)^{\alpha} - [(k-1)\Delta t]^{\alpha}\}}{\Delta y} Jn_{1,1}^{k} \quad (16)$$

Since two boundaries have been given, we only need discrete boundaries $x = 0$, $y = 0$ and the corner point (0,0).

Discretization scheme of Je and Jn

According to eq. (10), when $1 \le i \le N_x, 1 \le j \le N_{y+1}$, the solution scheme of *Je* is obtained:

$$Je_{i,j}^{k+1} = Je_{i,j}^{k} - \frac{\Delta t}{\tau_1}\left[Je_{i,j}^{k} + \frac{P_{i+1,j}^{k} - P_{i,j}^{k}}{\Delta x} H(y_i) \right] \quad (17)$$

where

$$H(y_i) = \begin{cases} \dfrac{2}{\Delta y}, & y_i \in \left[0, \dfrac{\Delta y}{2}\right] \\ 0, & \text{otherwise} \end{cases} \quad (18)$$

And based on eq. (11), when $1 \le i \le N_{x+1}, 1 \le j \le N_y$, the solution scheme of *Jn* is:

$$Jn_{i,j}^{k+1} = Jn_{i,j}^{k} - \frac{\Delta t}{\tau_2}\left(Jn_{i,j}^{k} + \frac{P_{i,j+1}^{k} - P_{i,j}^{k}}{\Delta y} \right) \quad (19)$$

Discretization scheme of initial conditions

According to eq. (12), when $t = 0$, the initial condition for *P* is:

$$P_{1,1}^{1} = \frac{1}{2V}, \quad \text{where } V = \frac{\Delta x \Delta y}{4}$$

And the initial condition for *J* is, $Je_{i,j}^{1} = Jn_{i,\mathrm{j}}^{1} = 0$.

Verification of numerical solution

In this section, we consider the particular case $\alpha = 1$ to verify the numerical solution. It is noted that when $\alpha = 1$, eqs. (8)-(10) become Cattaneo diffusion equation with anisotropic relaxation. We apply the Laplace transform and separation variable method to get the analytical solution to describe the particle distribution and mean square displacement (MSD). The particle distribution on the backbone is represented by Fox H-function.

When $\alpha = 1$, by performing the Laplace transform [20] for the time derivative in eqs. (8)-(10), we have:

$$s\bar{P} = -\frac{\partial \bar{J}_x}{\partial x} - \frac{\partial \bar{J}_y}{\partial y} + \delta(x)\delta(y) \quad (20)$$

$$\bar{J}_x + s\tau_1 \bar{J}_x = -\frac{\partial \bar{P}}{\partial x}\delta(y) \tag{21}$$

$$\bar{J}_y + s\tau_1 \bar{J}_y = -\frac{\partial \bar{P}}{\partial y} \tag{22}$$

where $\bar{P}(s,x,y)$ refers to the Laplace transform of $P(t,x,y)$, so do $\bar{J}_x(s,x,y)$ and $\bar{J}_y(s,x,y)$.

Equations (20)-(22) can be combined:

$$s\bar{P} = \frac{1}{1+s\tau_1}\frac{\partial^2 \bar{P}}{\partial x^2}\delta(y) + \frac{1}{1+s\tau_2}\frac{\partial^2 \bar{P}}{\partial y^2} + \delta(x)\delta(y) \tag{23}$$

Assuming that $\bar{P}(s,x,y) = f(s,x)e^{-\lambda|y|}$ [21], then:

$$\bar{P}(s,x,y=0) = f(s,x) \tag{24}$$

When $y \neq 0$, from eq. (23) we have:

$$s\bar{P} = \frac{\lambda^2}{1+s\tau_2}\bar{P} \tag{25}$$

The solution to λ is obtained:

$$\lambda = s^{1/2}(1+s\tau_2)^{1/2} \tag{26}$$

The P_1 is introduced in order to get the particle distribution on the backbone:

$$P_1(t,x) = \int_{-\varepsilon}^{+\infty} P(t,x,y)\,\mathrm{d}y \tag{27}$$

and yields:

$$P_1(s,x) = \frac{1}{s^{1/2}(1+s\tau_2)^{1/2}}[2 - \mathrm{e}^{-s^{1/2}(1+s\tau_2)^{1/2}\varepsilon}]f(s,x) \tag{28}$$

Integrating eq. (23) with respect to the variable *y*, we have:

$$sP_1(s,x) = \frac{1}{1+s\tau_1}\frac{\partial^2}{\partial x^2}f(s,x) + \delta(x) \tag{29}$$

From eqs. (28) and (29) we obtain the differential equation:

$$\frac{\partial^2}{\partial x^2}f(s,x) - s^{1/2}(1+s\tau_1)(1+s\tau_2)^{-1/2}[2 - \mathrm{e}^{-s^{1/2}(1+s\tau_2)^{1/2}\varepsilon}]f(s,x) = -(1+s\tau_1)\delta(x) \tag{30}$$

with the boundary condition is:

$$f(s,\pm\infty) = 0 \tag{31}$$

Letting $\varepsilon \to 0$, the solution of the equation is:

$$f(s,x)=\frac{1}{2}s^{-1/4}(1+s\tau_1)^{1/2}(1+s\tau_2)^{1/4}\mathrm{e}^{-s^{1/4}(1+s\tau_1)^{1/2}(1+s\tau_2)^{-1/4}|x|} \tag{32}$$

Then, the expression $\bar{P}(s,x,y)$ is:

$$\bar{P}(s,x,y)=\frac{1}{2}s^{-1/4}(1+s\tau_1)^{1/2}(1+s\tau_2)^{1/4}\mathrm{e}^{-[s^{1/4}(1+s\tau_1)^{1/2}(1+s\tau_2)^{-1/4}|x|+s^{1/2}(1+s\tau_2)^{1/2}|y|]} \tag{33}$$

For $y = 0$, the particle distribution on the backbone is obtained, we apply the Fox H-function [22] to describe the particle distribution on the backbone:

$$P(t,x,0)=L^{-1}\left[\frac{1}{2}s^{-1/4}(1+s\tau_1)^{1/2}(1+s\tau_2)^{1/4}\mathrm{e}^{-s^{1/4}(1+s\tau_1)^{1/2}(1+s\tau_2)^{-1/4}|x|}\right]=$$

$$=L^{-1}\left[\sum_{n=0}^{\infty}\frac{(-1)^n}{2n!}|x|^n\sum_{m=0}^{\infty}\frac{1}{m!}\tau_1{}^m\sum_{l=0}^{\infty}\frac{(-1)^l}{l!}(\tau_2 s)^l\frac{\Gamma\left(\frac{n+3}{2}\right)\Gamma\left(\frac{n-1}{4}+l\right)}{\Gamma\left(\frac{n-2m+3}{2}\right)\Gamma\left(\frac{n-1}{4}\right)}s^{\frac{n+4m-1}{4}}\right]=$$

$$=L^{-1}\left\{\sum_{n=0}^{\infty}\frac{(-1)^n}{2n!}|x|^n\sum_{m=0}^{\infty}\frac{1}{m!}\tau_1{}^m s^{-\frac{1-n-4m}{4}}H_{2,3}^{1,2}\left[\tau_2 s\middle|\begin{matrix}\left(1-\frac{n+3}{2},0\right),\left(1-\frac{n-1}{4},1\right)\\(0,1),\left(1-\frac{n-2m+3}{2},0\right),\left(1-\frac{n-1}{4},0\right)\end{matrix}\right]\right\}=$$

$$=\sum_{n=0}^{\infty}\frac{(-1)^n}{2n!}|x|^n\sum_{m=0}^{\infty}\frac{\tau_1{}^m}{m!t^{\frac{n+4m+3}{4}}}H_{3,3}^{1,2}\left[\frac{\tau_2}{t}\middle|\begin{matrix}\left(1-\frac{n+3}{2},0\right),\left(1-\frac{n-1}{4},1\right),\left(\frac{1-n-4m}{4},1\right)\\(0,1),\left(1-\frac{n-2m+3}{2},0\right),\left(1-\frac{n-1}{4},0\right)\end{matrix}\right] \tag{34}$$

where $H_{p,q}^{m,n}$ is the Fox H-function. In course of leading to eq. (34), the following expression of the Fox H-function is used:

$$H_{p,q+1}^{1,p}\left[z\middle|\begin{matrix}(1-a_1,\mathrm{A}_1),\cdots,(1-a_p,\mathrm{A}_p)\\(0,1),(1-b_1,B_1),\cdots,(1-b_q,B_q)\end{matrix}\right]=\sum_{n=0}^{\infty}\frac{(-z)^n\prod_{j=1}^{p}\Gamma(a_j+A_jn)}{n!\prod_{j=1}^{p}\Gamma(b_j+B_jn)} \tag{35}$$

By integrating with respect to x of the distribution function $P(t,x,0)$ on the interval $(-\infty,+\infty)$, we get the total number of particles on the x axis:

$$\langle P\rangle=\int_{-\infty}^{+\infty}P(t,x,0)\mathrm{d}x=2\frac{1}{2}L^{-1}\left[\int_{0}^{+\infty}s^{-1/4}(1+s\tau_1)^{1/2}(1+s\tau_2)^{1/4}e^{-s^{1/4}(1+s\tau_1)^{1/2}(1+s\tau_2)^{-1/4}x}\mathrm{d}x\right]=$$

$$=L^{-1}[s^{-1/2}(1+s\tau_2)^{1/2}] \tag{36}$$

Then the expression for the MSD is obtained:

$$\langle x^2(t)\rangle=\frac{\langle x^2P\rangle}{\langle P\rangle}=\frac{2L^{-1}[s^{-1}(1+s\tau_1)^{-1}(1+s\tau_2)]}{L^{-1}[s^{-1/2}(1+s\tau_2)^{1/2}]} \tag{37}$$

Finally, we can apply numerical Laplace inversion [23] to calculate MSD on the x axis.

We have obtained analytical and numerical solutions separately when $\alpha = 1$. The results are shown as follows, figs. 2 and 3, the curves of the analytical and numerical solutions are in good agreement.

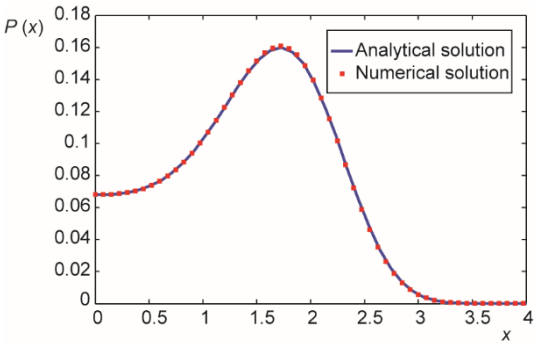

Figure 2. Comparison between numerical solution and analytical solution on the *x*-axis when $\tau_1 = 0.8$, $\tau_2 = 10^{-3}$, and $t = 1$

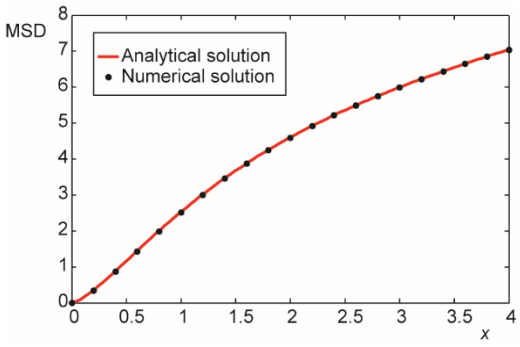

Figure 3. Comparison between numerical MSD and analytical MSD when $\tau_1 = 0.8$ and $\tau_2 = 10^{-3}$

Results and discussion

In this section, we discuss the dynamic characteristics of the spatial and temporal evolution of particle distribution and the MSD *vs.* time with the effects of involved parameters.

Figures 4 and 5 show the spatial evolution of particle distribution on the x axis with the effects of different τ. The influences of τ_1 on the particle distribution are shown in fig. 4. For $\tau_1 > \tau_2$, the distribution presents a wave form, and the larger the τ_1, the stronger the wave characteristic and more uneven the particle distribution. For $\tau_1 < \tau_2$, the distribution does not show the characteristics of the wave. The smaller τ_2 is, the higher the peak. The influences of τ_2 on the particle distribution are shown in fig. 5. The distribution changes from wave form to diffusion one gradually and the particles transport faster with the increase of parameter τ_2.

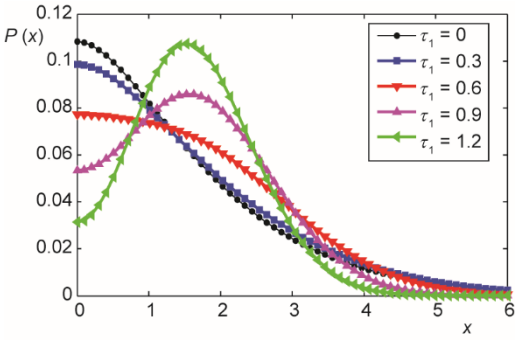

Figure 4. The spatial evolution of particle distribution on the *x*-axis with different τ_1 when $\tau_2 = 0.6$ and $t = 1$

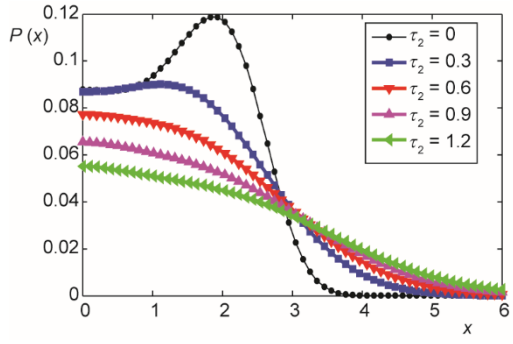

Figure 5. The spatial evolution of particle distribution on the *x*-axis with different τ_2 when $\tau_1 = 0.6$ and $t = 1$

Figures 6 and 7 indicate that the fractal dimension α has significant influence on particle distribution. When $\tau_1 > \tau_2$, the wave characteristics of the particle distribution gets

stronger as α increases. The smaller α is, the particle distribution more uniform is, and when $\tau_1 < \tau_2$, the distribution presents a diffusion form and the position of the peak declines with the decrease of α.

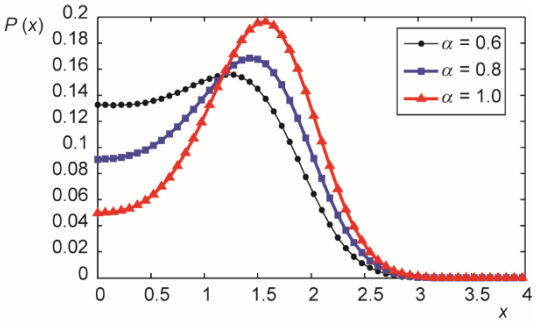

Figure 6. The spatial evolution of particle distribution on the *x*-axis with different α when $\tau_1 = 1$, $\tau_2 = 10^{-2}$, and $t = 1$

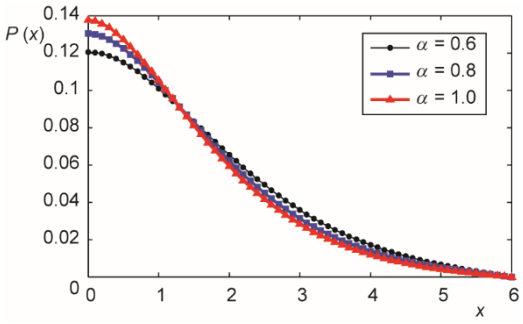

Figure 7. The spatial evolution of particle distribution on the *x*-axis with different α when $\tau_1 = 10^{-3}$, $\tau_2 = 0.1$, and $t = 1$

Figure 8 shows the effects of different τ_1 and τ_2 on MSD. In a long period, τ_1 and τ_2 have little effect on MSD. However, in a relatively short period of time, MSD decreases with the increase of τ_1 or the decrease of τ_2. That is to say, the relaxation parameter will affect the MSD in a short period, and the particle behavior becomes stable with time.

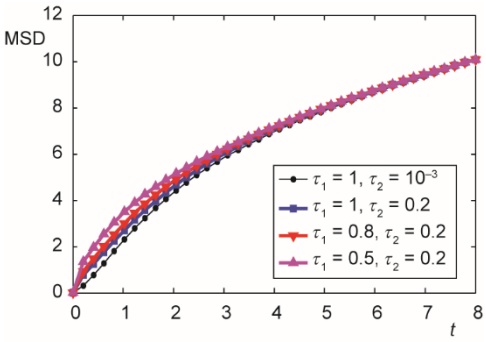

Figure 8. The temporal evolution of MSD on the *x*-axis with different τ_1 and τ_2 when $\alpha = 1$

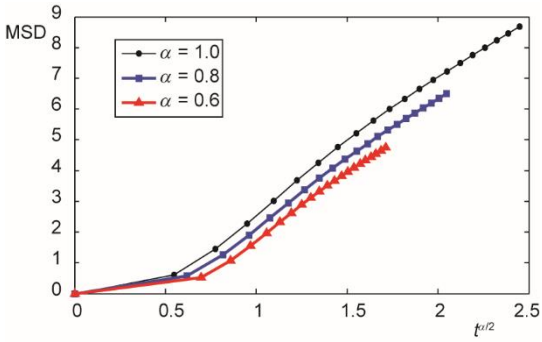

Figure 9. The temporal evolution of MSD on the *x*-axis with different α when $\tau_1 = 0.8$, $\tau_2 = 0.01$

Work obtained by other researchers shows that when $\alpha = 1$ and $t \to \infty$, MSD obeys the form of $t^{1/2}$ [24]. Since the fundamental solution of the Hausdorff derivative diffusion model is a stretched Gaussian distribution [14], the form of MSD in our model should be $t^{\alpha/2}$. Figure 9 confirms our inference which MSD~$t^{\alpha/2}$ when $t > \tau$. What is more, because the time fractal dimension $\alpha \leq 1$, the phenomena of diffusion discussed above belongs to sub-diffusion or heat transfer.

Conclusions

In this article, a Hausdorff fractal derivative is introduced to study the anomalous diffusion and heat transfer on a comb structure with anisotropic relaxation. The numerical so-

lution is obtained and the analytical solution is also given by Fox H-function in particular case, which verified the numerical solution.

Results show that the diffusion and heat transfer of particles is related to relaxation parameter and time fractal dimension. For $\tau_1 > \tau_2$, the distribution and heat transfer presents a wave form, and the larger τ_1, the stronger the wave characteristic. For $\tau_1 < \tau_2$, the distribution does not show the characteristics of the wave. In a relatively short period of time, MSD decreases with the increase of τ_1 or the decrease of τ_2. However, τ_1 and τ_2 have little effect on MSD in a long period. For time fractal dimension α, with the increase of the value of α, the particles are difficult to diffuse and heat transfer to a uniform concentration. The result of MSD shows that the diffusion and heat transfer form of the particle is sub-diffusion and heat transfer. Particularly, the MSD obeys the form of $t^{\alpha/2}$ when $t > \tau$.

Acknowledgment

The work is supported by the National Natural Science Foundations of China (Nos. 11772046, 81870345).

References

[1] Iomin, A., *et al.*, *Fractional Dynamics in Comb-Like Structures*, World Scientific, Singapore, 2018
[2] Baskin, E., Iomin, A., Superdiffusion on a Comb Structure, *Phys. Rev. Lett., 93* (2009), 12, pp. 120603
[3] Iomin, A., Superdiffusion of Cancer on a Comb Structure, *J. Phys. Conf. Ser., 7* (2005), 1, pp. 57-67
[4] Iomin, A., Toy Model of Fractional Transport of Cancer Cells Due to Self-Entrapping, *Phys. Rev. E, 73* (2006), 6, 061918
[5] Iomin, A., *et al.*, Reaction Front Propagation of Actin Polymerization in a Comb-Reaction System, *Chaos Soliton Fractals, 92* (2016), Nov., pp. 115-122
[6] Iomin, A., Richardson Diffusion in Neurons, *Phys. Rev. E, 100* (2019), 1, 010104
[7] Milovanov, A. V., Iomin, A., Subdiffusive Lévy Flights in Quantum Non-linear Schrödinger Lattices with Algebraic Power Non-linearity, *Phys. Rev. E, 99* (2019), 5, 052223
[8] Iomin, A., Subdiffusion on a Fractal Comb, *Phys. Rev. E, 83* (2011), 5, 052106
[9] Sandev, T., *et al.*, Fractional Diffusion on a Fractal Grid Comb, *Phys. Rev. E, 91* (2015), 3, 032108
[10] Korabel, N., Barkai, E., Paradoxes of Subdiffusive Infiltration in Disordered Systems, *Phys. Rev. Lett 104* (2010), 17, 170603
[11] Arkhincheev, V. E., *et al.*, Active Species in Porous Media: Random Walk and Capture in Traps, *Microelectronic Engineering, 88* (2011), 5, pp. 694-696
[12] Chen, W., Liang, Y. J., New Methodologies in Fractional and Fractal Derivatives Modeling, *Chaos Solitons Fractals, 102* (2017), Sept., pp. 72-77
[13] Cai, W., *et al.*, Three-Dimensional Hausdorff Derivative Diffusion Model for Isotropic/Anisotropic Fractal Porous Media, *Thermal Science, 22* (2018), Suppl. 1, pp. S1-S6
[14] Liang, Y. J., *et al.*, Distributed Order Hausdorff Derivative Diffusion Model to Characterize Non-Fickian Diffusion in Porous Media, Commun, *Non-linear Sci. Numer. Simul., 70* (2019), May, pp. 384-393
[15] Yang, X., *et al.*, A Local Structural Derivative PDE Model for Ultraslow Creep, *Comput. Math. Appl., 76* (2018), 7, pp. 1713-1718
[16] Qi, H. T., Guo, X. W., Transient Fractional Heat Conduction with Generalized Cattaneo Model, *Int. J Heat Mass Transfer, 76* (2014), Sept., pp. 535-539
[17] Compte, A., Metzler, R., The Generalized Cattaneo Equation for the Description of Anomalous Transport Processes, *J. Phys. A, 30* (1997), 21, pp. 7277-7289
[18] Cattaneo, C., Sulla Conduzione Del Calore, *Atti Sem. Mat. Fis. Univ. Modena, 3* (1948), pp. 83-101
[19] Fan, Y., *et al.*, Anomalous subdiffUsion in Angular and Radial Direction on a Circular Comb-Like Structure with Nonisotropic Relaxation, *Appl. Math. Model, 64* (2018), Dec., pp. 615-623
[20] Podlubny, I., *Fractional Differential Equation*, Academic Press, New York, USA, 1999
[21] Sandev, T., *et al.*, Heterogeneous Diffusion in Comb and Fractal Grid Structures, *Chaos. Solitons Fractals, 114* (2018), Sept., pp. 551-555

[22] Mathai, A. M., *et al., The H-Function: Theory and Applications,* Springer Science Business Media, New York, USA, 2009
[23] Brzezinski, D. W., Ostalczyk, P., Numerical Calculations Accuracy Comparison of the Inverse Laplace Transform Algorithms for Solutions of Fractional Order Differential Equations, *Non-linear Dyn., 84* (2016), 1, pp. 65-77
[24] Liu, L., *et al.,* Comb Model for the Anomalous Diffusion with Dual-Phase-Lag Constitutive Relation, Commun, *Non-linear Sci. Numer. Simul., 63* (2018), Oct., pp. 135-144

Paper submitted: January 13, 2020
Paper revised: March 2, 2020
Paper accepted: March 12, 2020